

Cu₂MnGeS₄ and Cu₄MnGe₂S₇: Two Polar Thiogermanates Exhibiting Second Harmonic Generation in the Infrared and Structures Derived from Hexagonal Diamond.

Jennifer R. Glenn,^a Jeong Bin Cho,^b Yiqun Wang,^c Andrew J. Craig,^a Jian-Han Zhang,^d Marvene Cribbs,^a Stanislav S. Stoyko,^a Christopher Barton,^a Allyson Bonnoni,^a Kate E. Rosello,^a Pedro Grima-Gallardo,^{e,f} Joseph H. MacNeil,^g James M. Rondinelli,^c Joon I. Jang,^{i,b} and Jennifer A. Aitken^{a*}

Supporting Information

Item	Page
Table S1. Crystal data, data collection and structure refinement details for Cu ₄ MnGe ₂ S ₇ .	S2
Table S2. Fractional atomic coordinates and isotropic or equivalent isotropic displacement parameters (Å ²) for Cu ₄ MnGe ₂ S ₇ .	S3
Table S3. Atomic displacement parameters (Å ²) for Cu ₄ MnGe ₂ S ₇ .	S3
Table S4. Bond distances (Å) for Cu ₄ MnGe ₂ S ₇ .	S4
Table S5. Bond angles (°) for Cu ₄ MnGe ₂ S ₇ .	S5
Table S6. Average bond distances (Å) and angles (°) for Cu ₄ MnGe ₂ S ₇ .	S6
Table S7. Extended connectivity table for Cu ₄ MnGe ₂ S ₇ used to predict structural distortions according to Pauling's second rule.	S7
Table S8. Bond valence sums, provided for each crystallographically unique ion, and global instability index (G) values for Cu ₂ MnGeS ₄ and Cu ₄ MnGe ₂ S ₇ .	S8
Table S9. The electronic bandgaps at different <i>k</i> -points using the PBE and HSE06 functional in Cu ₂ MnGeS ₄ .	S9
Table S10: The electronic bandgaps at different <i>k</i> -points using the PBE and HSE06 functional in Cu ₄ MnGe ₂ S ₇ .	S9
Figure S1. Simulated precession images for Cu ₄ MnGe ₂ S ₇ created using the single-crystal X-ray diffraction data. The (0kl), (h0l), and (hk0) planes in reciprocal space are shown from left to right, respectively. Sharp, bright spots are observed indicative of a single crystal.	S10
Figure S2. Differential thermal analysis diagrams for Cu ₂ MnGeS ₄ (top) and Cu ₄ MnGe ₂ S ₇ (bottom). Two cycles were conducted for each experiment.	S11
Figure S3. Attenuated total reflectance FT-IR data converted to transmittance for Cu ₂ MnGeS ₄ and Cu ₄ MnGe ₂ S ₇ .	S11

Table S1. Crystal data, data collection and structure refinement details for Cu₄MnGe₂S₇.

Formula weight	678.70
Crystal system, space group	Monoclinic, Cc (No.9)
Temperature (K)	296
<i>a</i> (Å)	16.7332(3)
<i>b</i> (Å)	6.47600(10)
<i>c</i> (Å)	9.8022(2)
β (°)	93.1517(9)
<i>V</i> (Å ³)	1060.60(3)
<i>Z</i>	4
<i>F</i> (000)	1268
Density g cm ⁻³	4.250
Radiation type	Mo Ka
μ (mm ⁻¹)	15.93
Crystal size (mm)	0.18 x 0.14 x 0.10
Crystal habit and color	Irregular polyhedron, black
Diffractometer	Bruker SMART Apex II
Radiation source	Fine-focus sealed tube
Absorption correction	Multi-scan, SADABS (Sheldrick, 2002)
No. of measured reflections	4396
No. of independent reflections	2405
No. of observed reflections [$>2\sigma(I)$]	2282
θ _{min} , θ _{max} (°)	2.4, 27.5
Completeness to θ=27.5°	100%
Limiting indices	-21 ≤ <i>h</i> ≤ 21 -8 ≤ <i>k</i> ≤ 8 -12 ≤ <i>l</i> ≤ 12
<i>R</i> _{int}	0.015
<i>R</i> [$F^2 > 2\sigma(F^2)$], w <i>R</i> (F^2), * <i>S</i>	0.021, 0.055, 1.07
(Δ/σ) _{max}	0.001
Extinction coefficient	0.00567 (18)
No. of data/restraints/parameters	0.70
Δρ _{max} , Δρ _{min} (e Å ⁻³)	-0.89
Absolute structure parameter (Flack parameter)	0.063 (12)

Table S2. Fractional atomic coordinates and isotropic or equivalent isotropic displacement parameters (\AA^2) for $\text{Cu}_4\text{MnGe}_2\text{S}_7$.

	<i>x</i>	<i>y</i>	<i>z</i>	$U_{\text{iso}}^*/U_{\text{eq}}$
Cu1	-0.00193 (6)	0.18000 (17)	-0.00131 (13)	0.0196 (3)
Cu2	0.06549 (5)	0.3393 (2)	0.36035 (14)	0.0190 (2)
Cu3	0.21237 (5)	0.3196 (2)	0.07988 (12)	0.0197 (3)
Cu4	0.35325 (4)	0.67831 (12)	0.28351 (9)	0.0186 (3)
Mn	0.28394 (8)	0.15156 (18)	0.43729 (12)	0.0143 (2)
Ge1	0.42802 (3)	0.16344 (7)	0.15672 (6)	0.00867 (19)
Ge2	0.63880 (4)	0.32497 (18)	0.22799 (10)	0.00879 (19)
S1	0.03322 (11)	0.16743 (19)	0.56571 (13)	0.0090 (3)
S2	0.17008 (10)	0.15178 (17)	0.27258 (13)	0.0118 (4)
S3	0.24068 (10)	0.6649 (2)	0.13736 (14)	0.0120 (4)
S4	0.32846 (10)	0.19229 (18)	-0.00212 (15)	0.0108 (3)
S5	0.39302 (10)	0.33995 (19)	0.33827 (13)	0.0107 (3)
S6	0.46156 (9)	0.16029 (18)	0.69731 (14)	0.0099 (4)
S7	0.60848 (10)	0.1666 (2)	0.41601 (15)	0.0106 (3)

Table S3. Atomic displacement parameters (\AA^2) for $\text{Cu}_4\text{MnGe}_2\text{S}_7$.

	U^{11}	U^{22}	U^{33}	U^{12}	U^{13}	U^{23}
Cu1	0.0179 (4)	0.0244 (4)	0.0164 (5)	-0.0028 (4)	0.0016 (3)	-0.0014 (3)
Cu2	0.0189 (5)	0.0167 (4)	0.0211 (4)	-0.0003 (3)	-0.0021 (3)	-0.0012 (3)
Cu3	0.0168 (5)	0.0216 (5)	0.0205 (5)	0.0016 (3)	-0.0001 (4)	-0.0003 (3)
Cu4	0.0183 (5)	0.0191 (4)	0.0186 (6)	-0.0008 (4)	0.0022 (4)	-0.0004 (3)
Mn	0.0127 (4)	0.0157 (4)	0.0144 (5)	0.0003 (5)	0.0006 (4)	-0.0003 (4)
Ge1	0.0075 (3)	0.0090 (3)	0.0094 (3)	0.0002 (3)	0.0000 (2)	-0.0009 (2)
Ge2	0.0086 (3)	0.0080 (2)	0.0096 (4)	0.0002 (2)	-0.0006 (2)	0.00001 (19)
S1	0.0076 (6)	0.0094 (5)	0.0100 (6)	0.0004 (5)	0.0008 (5)	-0.0012 (4)
S2	0.0140 (9)	0.0081 (6)	0.0132 (7)	-0.0005 (5)	0.0004 (6)	-0.0006 (4)
S3	0.0119 (10)	0.0111 (6)	0.0130 (6)	0.0017 (4)	0.0010 (6)	-0.0006 (4)
S4	0.0078 (8)	0.0140 (5)	0.0104 (5)	-0.0003 (5)	-0.0005 (5)	0.0018 (5)
S5	0.0115 (8)	0.0104 (6)	0.0102 (6)	0.0012 (4)	0.0020 (6)	-0.0016 (4)
S6	0.0104 (9)	0.0087 (5)	0.0108 (6)	-0.0007 (4)	0.0020 (6)	-0.0002 (4)
S7	0.0124 (9)	0.0101 (6)	0.0095 (5)	0.0002 (5)	0.0012 (6)	0.0011 (4)

Table S4. Bond distances (\AA) for $\text{Cu}_4\text{MnGe}_2\text{S}_7$.

Cu1—S7^{i}	2.2852 (18)	Cu4—S4^{v}	2.321 (2)
Cu1—S5^{i}	2.2969 (17)	Cu4—S5	2.3437 (16)
Cu1—S6^{i}	2.3161 (18)	Mn—S4^{vi}	2.4119 (17)
$\text{Cu1—S1}^{\text{ii}}$	2.4077 (14)	Mn—S2	2.429 (2)
$\text{Cu2—S7}^{\text{iii}}$	2.2942 (15)	Mn—S3^{v}	2.4371 (18)
Cu2—S6^{i}	2.2963 (16)	Mn—S5	2.441 (2)
Cu2—S2	2.3332 (19)	$\text{Ge1—S6}^{\text{ii}}$	2.2008 (13)
Cu2—S1	2.3879 (17)	Ge1—S5	2.2207 (14)
Cu3—S4	2.2959 (17)	Ge1—S4	2.2247 (15)
Cu3—S7^{i}	2.3029 (16)	$\text{Ge1—S1}^{\text{vii}}$	2.2949 (16)
Cu3—S2	2.3230 (18)	Ge2—S7	2.1930 (14)
Cu3—S3	2.348 (2)	$\text{Ge2—S2}^{\text{viii}}$	2.2179 (15)
$\text{Cu4—S6}^{\text{iv}}$	2.2933 (18)	$\text{Ge2—S3}^{\text{ix}}$	2.2218 (16)
Cu4—S3	2.3046 (16)	$\text{Ge2—S1}^{\text{vii}}$	2.3120 (15)

Symmetry codes: (i) $x-1/2, -y+1/2, z-1/2$; (ii) $x, -y, z-1/2$; (iii) $x-1/2, y+1/2, z$; (iv) $x, -y+1, z-1/2$; (v) $x, -y+1, z+1/2$; (vi) $x, -y, z+1/2$; (vii) $x+1/2, -y+1/2, z-1/2$; (viii) $x+1/2, y+1/2, z$; (ix) $x+1/2, y-1/2, z$; (x) $x-1/2, -y+1/2, z+1/2$; (xi) $x-1/2, y-1/2, z$; (xii) $x+1/2, -y+1/2, z+1/2$.

Table S5. Bond angles ($^{\circ}$) for $\text{Cu}_4\text{MnGe}_2\text{S}_7$.

$\text{S}7^{\text{i}}$ — Cu1 — $\text{S}5^{\text{i}}$	112.64 (8)	Ge1^{x} — S1 — Ge2^{x}	107.21 (6)
$\text{S}7^{\text{i}}$ — Cu1 — $\text{S}6^{\text{i}}$	111.09 (5)	Ge1^{x} — S1 — Cu2	108.61 (5)
$\text{S}5^{\text{i}}$ — Cu1 — $\text{S}6^{\text{i}}$	111.91 (7)	Ge2^{x} — S1 — Cu2	111.74 (10)
$\text{S}7^{\text{i}}$ — Cu1 — $\text{S}1^{\text{ii}}$	108.24 (7)	Ge1^{x} — S1 — Cu1^{vi}	111.78 (8)
$\text{S}5^{\text{i}}$ — Cu1 — $\text{S}1^{\text{ii}}$	107.49 (5)	Ge2^{x} — S1 — Cu1^{vi}	111.93 (6)
$\text{S}6^{\text{i}}$ — Cu1 — $\text{S}1^{\text{ii}}$	105.05 (8)	Cu2 — S1 — Cu1^{vi}	105.59 (7)
$\text{S}7^{\text{iii}}$ — Cu2 — $\text{S}6^{\text{i}}$	112.34 (6)	Ge2^{x} — S2 — Cu3	111.43 (7)
$\text{S}7^{\text{iii}}$ — Cu2 — $\text{S}2$	109.68 (7)	Ge2^{x} — S2 — Cu2	113.31 (9)
$\text{S}6^{\text{i}}$ — Cu2 — $\text{S}2$	107.38 (8)	Cu3 — S2 — Cu2	108.93 (6)
$\text{S}7^{\text{iii}}$ — Cu2 — $\text{S}1$	108.22 (9)	Ge2^{x} — S2 — Mn	107.37 (6)
$\text{S}6^{\text{i}}$ — Cu2 — $\text{S}1$	112.92 (7)	Cu3 — S2 — Mn	106.14 (9)
$\text{S}2$ — Cu2 — $\text{S}1$	106.09 (5)	Cu2 — S2 — Mn	109.40 (7)
$\text{S}4$ — Cu3 — $\text{S}7^{\text{i}}$	112.99 (9)	Ge2^{iii} — S3 — Cu4	110.65 (7)
$\text{S}4$ — Cu3 — $\text{S}2$	114.71 (6)	Ge2^{iii} — S3 — Cu3	113.03 (9)
$\text{S}7^{\text{i}}$ — Cu3 — $\text{S}2$	109.47 (7)	Cu4 — S3 — Cu3	109.41 (5)
$\text{S}4$ — Cu3 — $\text{S}3$	105.22 (6)	Ge2^{iii} — S3 — Mn^{iv}	111.25 (7)
$\text{S}7^{\text{i}}$ — Cu3 — $\text{S}3$	105.37 (7)	Cu4 — S3 — Mn^{iv}	102.30 (8)
$\text{S}2$ — Cu3 — $\text{S}3$	108.48 (9)	Cu3 — S3 — Mn^{iv}	109.66 (7)
$\text{S}6^{\text{iv}}$ — Cu4 — $\text{S}3$	115.07 (6)	Ge1 — S4 — Cu3	113.62 (7)
$\text{S}6^{\text{iv}}$ — Cu4 — $\text{S}4^{\text{v}}$	110.68 (6)	Ge1 — S4 — Cu4^{iv}	119.99 (8)
$\text{S}3$ — Cu4 — $\text{S}4^{\text{v}}$	113.32 (7)	Cu3 — S4 — Cu4^{iv}	112.59 (6)
$\text{S}6^{\text{iv}}$ — Cu4 — $\text{S}5$	106.88 (6)	Ge1 — S4 — Mn^{ii}	107.70 (5)
$\text{S}3$ — Cu4 — $\text{S}5$	108.61 (6)	Cu3 — S4 — Mn^{ii}	99.32 (10)
$\text{S}4^{\text{v}}$ — Cu4 — $\text{S}5$	101.12 (6)	Cu4^{iv} — S4 — Mn^{ii}	100.29 (7)
$\text{S}4^{\text{vi}}$ — Mn — $\text{S}2$	112.62 (7)	Ge1 — S5 — Cu1^{xii}	107.10 (8)
$\text{S}4^{\text{vi}}$ — Mn — $\text{S}3^{\text{v}}$	110.71 (8)	Ge1 — S5 — Cu4	112.44 (7)
$\text{S}2$ — Mn — $\text{S}3^{\text{v}}$	106.13 (7)	Cu1^{xii} — S5 — Cu4	113.98 (6)
$\text{S}4^{\text{vi}}$ — Mn — $\text{S}5$	109.38 (7)	Ge1 — S5 — Mn	107.30 (5)
$\text{S}2$ — Mn — $\text{S}5$	108.17 (7)	Cu1^{xii} — S5 — Mn	105.10 (6)
$\text{S}3^{\text{v}}$ — Mn — $\text{S}5$	109.75 (6)	Cu4 — S5 — Mn	110.45 (8)
$\text{S}6^{\text{ii}}$ — Ge1 — $\text{S}5$	114.92 (6)	Ge1^{vi} — S6 — Cu4^{v}	107.58 (7)
$\text{S}6^{\text{ii}}$ — Ge1 — $\text{S}4$	112.35 (5)	Ge1^{vi} — S6 — Cu2^{xii}	107.62 (6)
$\text{S}5$ — Ge1 — $\text{S}4$	107.29 (6)	Cu4^{v} — S6 — Cu2^{xii}	109.07 (6)
$\text{S}6^{\text{ii}}$ — Ge1 — $\text{S}1^{\text{vii}}$	109.36 (6)	Ge1^{vi} — S6 — Cu1^{xii}	110.48 (7)
$\text{S}5$ — Ge1 — $\text{S}1^{\text{vii}}$	107.92 (5)	Cu4^{v} — S6 — Cu1^{xii}	110.89 (6)
$\text{S}4$ — Ge1 — $\text{S}1^{\text{vii}}$	104.40 (6)	Cu2^{xii} — S6 — Cu1^{xii}	111.09 (8)
$\text{S}7$ — Ge2 — $\text{S}2^{\text{viii}}$	110.10 (9)	Ge2 — S7 — Cu1^{xii}	108.88 (6)
$\text{S}7$ — Ge2 — $\text{S}3^{\text{ix}}$	109.62 (6)	Ge2 — S7 — Cu2^{ix}	108.44 (8)
$\text{S}2^{\text{viii}}$ — Ge2 — $\text{S}3^{\text{ix}}$	110.25 (7)	Cu1^{xii} — S7 — Cu2^{ix}	103.71 (10)
$\text{S}7$ — Ge2 — $\text{S}1^{\text{vii}}$	112.63 (8)	Ge2 — S7 — Cu3^{xii}	111.55 (12)
$\text{S}2^{\text{viii}}$ — Ge2 — $\text{S}1^{\text{vii}}$	106.16 (6)	Cu1^{xii} — S7 — Cu3^{xii}	109.25 (7)
$\text{S}3^{\text{ix}}$ — Ge2 — $\text{S}1^{\text{vii}}$	108.00 (8)	Cu2^{ix} — S7 — Cu3^{xii}	114.62 (7)

Symmetry codes: (i) $x-1/2, -y+1/2, z-1/2$; (ii) $x, -y, z-1/2$; (iii) $x-1/2, y+1/2, z$; (iv) $x, -y+1, z-1/2$; (v) $x, -y+1, z+1/2$; (vi) $x, -y, z+1/2$; (vii) $x+1/2, -y+1/2, z-1/2$; (viii) $x+1/2, y+1/2, z$; (ix) $x+1/2, y-1/2, z$; (x) $x-1/2, -y+1/2, z+1/2$; (xi) $x-1/2, y-1/2, z$; (xii) $x+1/2, -y+1/2, z+1/2$.

Table S6. Average bond distances (\AA) and angles ($^\circ$) for $\text{Cu}_4\text{MnGe}_2\text{S}_7$.

	Average bond distance (\AA)		Average bond angle ($^\circ$)
Cu1-S	2.326(3)	S-Cu1-S	109.4(2)
Cu2-S	2.328(3)	S-Cu2-S	109.4(2)
Cu3-S	2.317(4)	S-Cu3-S	109.4(2)
Cu4-S	2.316(4)	S-Cu4-S	109.3(2)
All Cu-S	2.322(7)	S-Ge1-S	109.4(1)
Ge1-S	2.235(3)	S-Ge2-S	109.5(2)
Ge2-S	2.236(3)	S-Mn-S	109.5(2)
All Ge-S	2.236(4)	All S-Cu-S	109.4(3)
Ge-S (short)*	2.213(4)	All S-Ge-S	109.4(2)
Mn-S	2.430(4)	S-Cu1-S	109.4(2)
S1-M	2.351(3)		
S2-M	2.326(4)		
S3-M	2.328(4)		
S4-M	2.313(3)		
S5-M	2.326(3)		
S6-M	2.277(3)		
S7-M	2.269(3)		
All S-M	2.313(9)		

*The short Ge-S bond average excludes the Ge1-S1 and Ge2-S1 bonds.

Table S7. Extended connectivity table for $\text{Cu}_4\text{MnGe}_2\text{S}_7$ used to predict structural distortions according to Pauling's second rule. When the charge on the sulfur is compensated (CMP) by the cations in its first coordination sphere the coordination polyhedron is regular. When the charge of the sulfur is over CMP or under CMP cation-anion bonds will lengthen and shorten, respectively.

		Anions							Horizontal Bond Strength Sums
		S1	S2	S3	S4	S5	S6	S7	
Cations	Cu1	$\frac{1}{4}$				$\frac{1}{4}$	$\frac{1}{4}$	$\frac{1}{4}$	$\Sigma = 1$
	Cu2	$\frac{1}{4}$	$\frac{1}{4}$				$\frac{1}{4}$	$\frac{1}{4}$	$\Sigma = 1$
	Cu3		$\frac{1}{4}$	$\frac{1}{4}$	$\frac{1}{4}$			$\frac{1}{4}$	$\Sigma = 1$
	Cu4			$\frac{1}{4}$	$\frac{1}{4}$	$\frac{1}{4}$	$\frac{1}{4}$		$\Sigma = 1$
	Mn		$\frac{2}{4}$	$\frac{2}{4}$	$\frac{2}{4}$	$\frac{2}{4}$			$\Sigma = 2$
	Ge1	$\frac{4}{4}$			$\frac{4}{4}$	$\frac{4}{4}$	$\frac{4}{4}$		$\Sigma = 4$
	Ge2	$\frac{4}{4}$	$\frac{4}{4}$	$\frac{4}{4}$				$\frac{4}{4}$	$\Sigma = 4$
	Vertical Bond Strength Sums	$\Sigma = 2.5$ $2.5 > 2$	$\Sigma = 2$	$\Sigma = 2$	$\Sigma = 2$	$\Sigma = 2$	$\Sigma = 1.75$ $1.75 < 2$	$\Sigma = 1.75$ $1.75 < 2$	
Charge compensation		OVER CMP	CMP	CMP	CMP	CMP	UNDER CMP	UNDER CMP	

Table S8. Bond valence sums, provided for each crystallographically unique ion, and global instability index (G) values for $\text{Cu}_2\text{MnGeS}_4$ and $\text{Cu}_4\text{MnGe}_2\text{S}_7$.

Compound	Space Group	Bond Valence Sums				G values	Structure Reference
		Cu ⁺	Mn ^{2+*}	Ge ⁴⁺	S ²⁻		
$\text{Cu}_2\text{MnGeS}_4$	$Pmn2_1$	(4b) 1.26	(2a) 2.04	(2a) 3.89	S1(2a) 2.04 S2(2a) 2.07 S3(4b) 2.22	0.18	T. Bernert, A. Pfitzner, <i>Z. Kristallogr.</i> , 2005, 220 , 968-972.
$\text{Cu}_4\text{MnGe}_2\text{S}_7$	<i>Cc</i>	(4a) Cu1 1.27 Cu2 1.26 Cu3 1.29 Cu4 1.30	(4a) 2.15	(4a) Ge1: 3.82 Ge2: 3.82	(4a) S1 2.10 S2 2.16 S3 2.14 S4 2.20 S5 2.15 S6 2.05 S7 2.10	0.19	This work

R_0 and b values come from https://www.iucr.org/_data/assets/file/0011/150779/bvparm2020.cif

*The R_0 values were used for the specific oxidation states of the ions except for Mn²⁺, which has an “unchecked”/unreliable R_0 value. In the case of Mn, we used the value for the unspecified oxidation state, $R_0=2.20 \text{ \AA}$, which can also be found in the following reference: N. E. Brese, M. O’Keeffe, *Acta Cryst.* 1991, **B47**, 192-197.

Table S9. The electronic bandgaps at different k -points using the PBE and HSE06 functional in $\text{Cu}_2\text{MnGeS}_4$.

K-point	E_g^{PBE} (eV)	E_g^{HSE06} (eV)	ΔE_g (eV)
(0, 0, 0)	0.6	1.9	1.3
(1/2, 0, 0)	1.3	3	1.7
(1/2, 1/2, 0)	1.8	3.4	1.6
(0, 1/2, 0)	0.8	2.2	1.4
(0, 0, 1/2)	0.8	2.3	1.5
(1/2, 0, 1/2)	1.4	3.1	1.7
(1/2, 1/2, 1/2)	1.7	3.2	1.5

Table S10: The electronic bandgaps at different k -points using the PBE and HSE06 functional in $\text{Cu}_4\text{MnGe}_2\text{S}_7$.

K-point	E_g^{PBE} (eV)	E_g^{HSE06} (eV)	ΔE_g (eV)
(0, 0, 0)	0.5	1.7	1.2
(1/2, 0, 0)	0.8	2.1	1.3
(0, 1/2, 0)	0.9	2.3	1.4
(1/2, 1/2, 0)	0.9	2.3	1.4
(1/2, 1/2, 1/3)	1	2.2	1.2
(0, 1/2, 1/3)	1.1	2.4	1.3
(1/2, 1/2, 1/3)	1	2.3	1.3

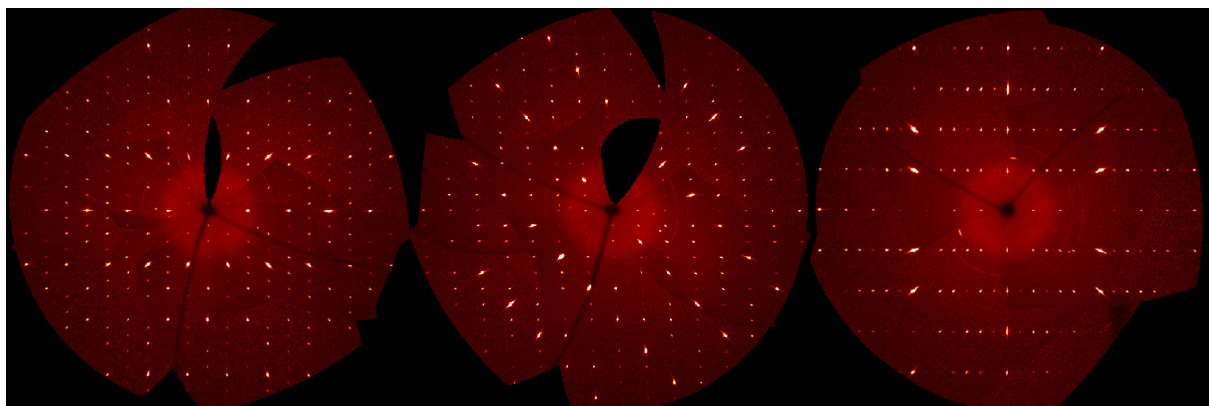


Figure S1. Simulated precession images for $\text{Cu}_4\text{MnGe}_2\text{S}_7$ created using the single-crystal X-ray diffraction data. The $(0kl)$, $(h0l)$, and $(hk0)$ planes in reciprocal space are shown from left to right, respectively. Sharp, bright spots are observed indicative of a single crystal.

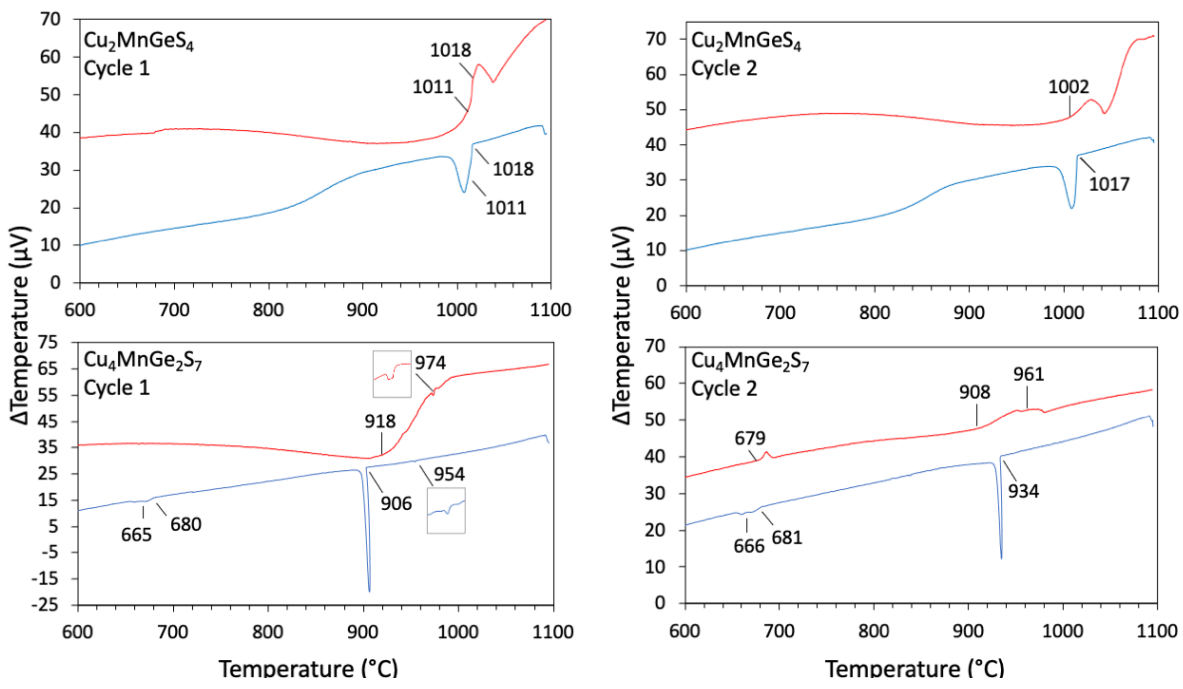


Figure S2. Differential thermal analysis diagrams for $\text{Cu}_2\text{MnGeS}_4$ (top) and $\text{Cu}_4\text{MnGe}_2\text{S}_7$ (bottom). Two cycles were conducted for each experiment.

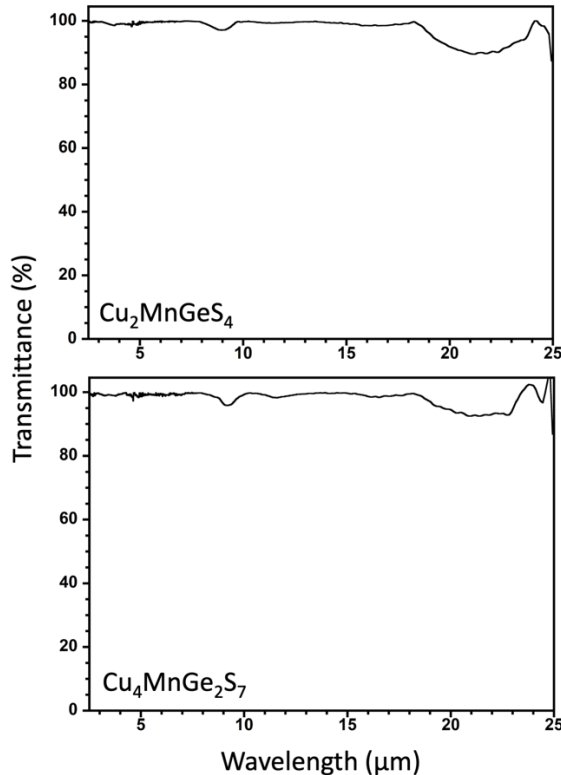


Figure S3. Attenuated total reflectance FT-IR data converted to transmittance for $\text{Cu}_2\text{MnGeS}_4$ and $\text{Cu}_4\text{MnGe}_2\text{S}_7$.